SECRET

SECURITY NO. 62-2911-61
COPY 5 OF 6 COPIES
11 PAGES

Encl. #1 to
OXC 1519
COPY 4 OF 4

PROGRESS REPORT - 2/16/61 - 3/15/61

CONTRACT NO. AF 33(600)40280

SYSTEM

Type designation AN/APQ-93 has been assigned to the SOARD equipment.

Platform stability requirements have been computed and are outlined in RTM 210 which is attached. The conclusion differs slightly from those previously reported. Design requirements are unchanged however.

Study of an accelerometer system for measuring and correcting the effects of platform instability has been initiated. Preliminary results indicate that the accelerometer can be located in the same region as the equipment, rather than at the antenna as previously believed.

The initial antenna design to this reporting period had an integral radome as part of the antenna structure. There is reason to believe that such a "flush" antenna could not be suitably sealed to the skin of the aircraft for the type of conditions included in the design requirements. Accordingly, a separate (1/8" fiberglass) radome is under consideration. The structural ramifications are being investigated.

Test philosophy has been given some thought. The mechanical requirements of the railroad and railroad range are under study. It appears that a careful evaluation of the trade-off of complexity should be made. It seems that essentially the same accomplishments could be achieved using simulated targets in a much more versatile manner.

Modifications to the system parameters as required by flight test in a vehicle such as the F101 have been considered and some initial conclusions are included in Addendum #1 (Scaling APQ-93 Parameters). Effect of such flight test upon the recorder are yet to be investigated.

SECRET

The power distribution diagram has been completed, including system control functions.

SYNCHRONIZER

Frequency Generator

A design specification has been given to drafting. General layout work is being done. This unit will be divided into three chassis; a fixed frequency multiplier, a variable oscillator-multiplier and an IF-DC amplifier.

A breadboard of the variable oscillator multiplier chassis similar to the end-use package is 60% constructed and checked out.

Components are being mounted on the same kind of breadboard for the fixed frequency multiplier. Both of these units are being built in an effort to make the chassis more compact, without the sacrifice of serviceability. One of the frequency mixers and the multivibrators have been checked out. Work is also being done on the D.C. amplifier and the other mixer.

The status of CHPO2 oscillator-discriminator unit which is supplied by Bulova Watch Company is as follows: The breadboard unit delivery date is 5-1-61 and the two prototypes are to be here on 5-8-61. The suitability of the design cannot be established until these units are in hand.

Sync-Generator

A design specification has been given to Drafting. Drawings for this assembly are about 60% complete.

A model of the printed board assembly to be used in the final units has been completed and checked out. It is now being checked over the required temperature range. The circuit operation is normal at high temperature, but there are still problems at temperatures below 0 deg. C.

The CHPO1 oscillator units on order are virtually finished except that the supplier is waiting for the crystals. The promise date for the breadboard and two prototypes is 4-24-61. This is not felt to be a critical item.

The jitter tester available to measure pulse jitter would not accept the pulse widths of our design. However it has been established that what jitter there is is below acceptable levels.

STALO ASSEMBLY

A D.C. amplifier with a differential input stage has been built and checked out. Drifts for a duration of several seconds are approximately one millivolt with respect to the input. Six millivolts drift will produce 100 cps deviation when loop is closed. Furthermore the deviation is well below limits when the power supply voltage deviations are around 1%. A frequency deviation in modulating frequency has not been taken with this amplifier in the stalo loop.

A design specification indicating modifications to be made on the present Bomare Microwave Oscillator has been turned into Drafting. Information concerning the additional R.F. components; namely directional coupler, attenuator, crystal modulator, receiver mixer, buffer amplifier and interconnecting waveguide has been included in the D-spec. Layout work has begun. Drawings listing the long lead items have been made and will soon be released to the Model Shop.

Three STALO units will be provided by the shop from an existing production run beginning in May. These will be modified per above.

NAVIGATION TIE-IN

A breadboard consisting of a servo amplifier, geared motor and two synchro resolvers has been built and checked out. Gears; bearings, etc have been ordered and will be incorporated between the resolver and one precision potentiometer which is due the first part of April.

Negotiations have been made with Bowmar Instrument Corporation to manufacture a gear box for the ground speed step servo motor and then assemble the motor and a precision potentiometer to the gear box.

A design specification has been written and turned in to Drafting. Layout work has begun.

RECEIVER

The first TWT was received and under test was found to be defective. It was returned. Another was promised 3/17/61 and is to be an engineering model.

Construction of the IF amplifier has begun and is about 50% complete. Electrical test will begin week of 3/27/61.

A reduction in amplitude of video signals resulted in a review of the video amplifier design. Transistors were considered but because of time, expense and maintenance difficulties associated with the type of circuits involved it was decided to continue to use vacuum tube.

The redesign of the video amplifier and automatic gain stabilization circuit is about 95% complete. Mechanical layout is about 80% complete and drawings for fabrication of the chassis are currently being drawn.

Work is still continuing on the design of a suitable synchronous mixer at 120 mcs. Two types of balanced mixers have been designed with both showing only marginal operation. At the present time the balanced mixer using ceramic triodes shows the most promise and a suitable design is about 60% complete.

POWER SUPPLY AND CONTROL

A review of the quotations received for the design and construction of regulated power supplies resulted in the decision to have the components section design and manufacture the power supply subassemblies per E-1806, Revision C. The ambient temperature surrounding these subassemblies will be a minimum of 0°C and a maximum of 40°C.

MODULATOR

Drafting has completed the layout of the modulator and is proceeding with the detail drawings. Release to shop is expected two weeks ahead of schedule.

Tests of the breadboard modulator have been made as far as possible with the parts available.

SECRET

Burmac is progressing satisfactorily with the PFN and pulse transformer. The design is complete and the first model is now being constructed. It is expected that this model will be ready for checkout in the breadboard modulator April 1.

Raytheon has a promise of May for a low capacity filament transformer. In the mean time a lab type will be used for tests. Final proof of design however will have to await this item.

RESONANT RING DUPLEXER

The design and breadboarding of a pulse detection circuit for final system use was begun.

The following data was taken with pressurized switches:

Pressure	Ring Power (Peak)	Rise Time
30 psig	320 KW	3.5 nsec
45 psig	450 KW	6 nsec

Airtron, when contacted in reference to ring for Westinghouse, stated they were having problems generating pure (lossless) TE_{01} circular mode from rectangular to circular input coupler. Information was also received that the delivery of the SEI ring has been delayed by 30 days. Westinghouse will not be quoted until April 1.

Requests for quotes for the dump switches were sent to five suppliers. Four did no quote. Microwave Associates is still looking at the problem, but it seems doubtful that a quote will be received.

SWITCH TUBES

Since the last period additional tests were made with the tube containing a trigger electrode. The sampling scope was used in these tests to obtain a more accurate measurement of the breakdown times that were being observed. It was noted that for high pressures (i.e. pressures greater than that required to prevent R.F. breakdown at 250 KW resulting in lower hold off

SECRET

powers) the rise time or switching time was much faster. A switching time of about 5 nanoseconds was measured once before the tube developed a leak.

The results of these tests indicated that it was possible to hold off R.F. breakdown at 250 KW and to initiate rapid breakdown with the application of an external voltage pulse. However, it was also shown that a redesign of the tube was needed particularly with respect to obtaining a bakeable tube and one with variable electrodes. Having obtained preliminary information on this type of tube and because of the redesign necessary, it has been decided to temporarily forego work on this tube in order to evaluate the magnetic switching technique that was proposed. Components and tubes have been built for this and are currently being set up for high power tests. Some calculations were made in an attempt to predict breakdown time of the magnetic device. The time calculated was in the order of 300 nanoseconds. Because of the approximations made in the computation, this figure is worth checking experimentally to determine whether an order of magnitude improvement can be obtained.

A simple, thin walled tube containing a glass capsule has been assembled and low level tested for use in investigation of WX-4641 requirements. This, too, will be a low pressure device with a plasma that is broken down by an applied magnetic field. It will be necessary to time share existing equipment in order to test tubes on both programs.

ANTENNA

Electrical

103 Manifold - Work is continuing on the various transition and miter corner sections. Much difficulty has been experienced in some of these pieces because of the extreme waveguide aspect ratios and machining and fabrication difficulties. Tentative dimensions have been compiled for both manifolds and power dividers.

104 Array - A second array "stick" (11" long) was made with corrected slot spacing and conductance in an attempt to eliminate the "image lobe" which was obtained with the first stick design (19" long). Radiation patterns for this stick have been measured and found to conform closely to the theoretical patterns in the shaped region. In addition, the image lobe is now -10 db, which is definitely encouraging when compared to the results of the 19" design. Work is continuing to reduce the image lobe amplitude and to correct for mutual coupling effects of overlapping slots.

106 - Radome - Dielectric measurements on various samples were completed and dielectric and transmission data compiled in chart form.

107 - Load - Evaluation of both full and half-height load samples has verified the load material and design. However, as this item is released, mounting requirements must be specified and the manufacturer may have to make small corrections in the load design.

112 - Specification - The R-Spec has been brought up to date and retyped to correct the format.

Mechanical

202 Structure Analysis - The honeycomb beam outline was compared to a sketch of the antenna cavity as supplied by G Section and minor changes to the configuration were made to eliminate interference. The end use drawing of the honeycomb will be started during the week of March 15. Release to the Model Shop will be made as soon as the drawing is completed.

203 - Manifold Design - One of the two end use drawings was partially completed in Drafting. The second drawing, which is a mirror image of the first, will be started upon completion of the first. Technicraft has withdrawn its quote on the basis of the fact that the firm who would normally do its electro forming, has previously been approached and has made a quote directly to Westinghouse.

The pressure port, pressure windows and connecting tubing have been eliminated from the manifold design after it was established that a pressure drop in the antenna would not cause magnetron burn out.

204 - Array Design - The array mechanical design is complete with the exception of the exact location of the slots. The end use drawing will be started when the information is available. Tensile test specimens of electroformed nickel have been ordered and will be subjected to heat aging and high temperature tensile tests at the Research Lab. The objective of this test is to determine the probable tensile strength and yield strength of the electroformed nickel at 550 degrees F.

The mechanical design of the power dividers has been completed and end use drawings will be started by Drafting during the week of 3-15-61.

205 - Tolerance Study - Reduced operating pressure requirements have required another series of computer runs to determine the optimum honeycomb beam structure. The results of this study are that a honeycomb beam of 1.54" thickness, having faces .040" thick can be used without causing the sidelobes to exceed specification limits.

The weight of the antenna is estimated to be about 125 lbs.

206 - Radome Design - A slotted nickel waveguide has had a laminate sealing strip bonded to it and has been tested for air leakage at 550 degrees F. The leakage rate has been 1-1/2 to 2 psig per hour which is well below the prorated allowable leakage rate. Efforts are now being directed toward improving the bonding techniques, optimizing the cure time and maintaining reliability.

207 - Load and Seals - "O" Rings made from a high temperature compound have been ordered and will be tested when received.

The load design and mounting configuration has been completed and a purchase part drawing will be requested during the week of 3-15-61.

211 - Drafting - The antenna layout has been made and revised to reflect changes mentioned in tasks above. Detail and use dr wings will be started.

ADDENDUM #1
SCALING APQ-93 PARAMETERS

The quantities of importance in the APQ-93 system are:

a. Total range change in view, ΔR

b. Time of view t_v

c. Velocity of A/C V

d. Beamwidth B

e. Maximum doppler frequency, f_{dm}

f. Film velocity v

g. Range R

h. Length of beam intercept, L

i. Length of film record, ℓ

These quantities are related by the following relationships:

$$\Delta R = R\left(\sec\frac{B}{2} - 1\right) \sim \frac{RB^2}{8} \qquad (1)$$

$$L = 2R\tan\frac{B}{2} \sim RB \qquad (2)$$

$$f_{dm} = \frac{2V\sin B/2}{\lambda} \sim \frac{VB}{\lambda} \qquad (3)$$

$$t_v = \frac{L}{V} \qquad (4)$$

$$\ell = v\, t_v$$

Assume that it is desired to scale V by a factor of 0.45 and R by a factor of 0.5. In order to get identical pattern on the film, it is necessary to hold ℓ and Δ R constant.

Using primes to represent the scaled quantities,

$RB^2 = R^1 (B^1)^2$, or if $R^1 = 0.5R$ (6)

$B^1 = \sqrt{2}\ B$ (6a)

$L^1 = R^1 B^1 = 0.5R \cdot \sqrt{2}\ B = \frac{L}{\sqrt{2}}$ (7)

$t_v^1 = \frac{L^1}{V^1} = \frac{L}{\sqrt{2} \times .45V} = 1.56\ t_v$ (8)

$= v\ t_v = v^1\ t_v^1 . = v^1 .\ 1.56\ t_v$ (9)

$v^1 = 0.64\ v.$ (9a)

$$f_d^1 = \frac{V^1 B^1}{\lambda} = \frac{.45V \times \sqrt{2}\ B}{\lambda} = .64\ f_d$$

Therefore, as expected, there is no difficulty in recording. The film runs at 0.64 speed, and the maximum dop ler is 0.64 normal.

Note, however, that this compensation can be had at only one range, since the true R vs the R displayed by the processor would be different (no interlacing). By a substitution of conical lenses, a match could be obtained.

OXC 1579
COPY 4 OF 4

ABSTRACT

REPORT NO. WSTM #210 DATE Feb. 28, 1961 PAGES 21

TITLE STABILITY REQUIREMENTS FOR A SIDE-LOOKING DOPPLER RADAR

CLASSIFICATION: REPORT SECRET ABSTRACT* Unclassified

ABSTRACT:

The average pattern is determined for a linear antenna with a random phase disturbance. This result is employed to establish platform and STALO stability requirements limiting side lobe magnitudes and main beam deterioriation to selected levels. Curves of allowable platform motion and STALO frequency modulation are given for several cases.

UNITERMS

STALO
Stability
Side-looking
Doppler

AUTHOR(S)

25X1

*ABSTRACT SHOULD BE UNCLASSIFIED IF AT ALL POSSIBLE

AE65A

Security No. 62-2842-61
Pages 21
Copy 8 of 10 Copies

Abstract

The average pattern is determined for a linear antenna with a random phase disturbance. This result is employed to establish platform and STALO stability requirements limiting side lobe magnitudes and main beam deterioriation to selected levels. Curves of allowable platform motion and STALO frequency modulation are given for several cases.

STABILITY REQUIREMENTS FOR A SIDE-LOOKING DOPPLER RADAR

Introduction

Instability of the platform or the STALO represents one of the most serious degrading factors in a side-looking, doppler radar. This memorandum will develop tentative specifications for stability requirements in this type of system.

The basic problem is that of determining the pattern of a wrinkled or bent linear antenna. Or, it may be thought of as determining the effect of a wrinkled wave front. In the case of a side-looking doppler radar, the platform motion or the STALO phase shift is developed as a function of time. However, since the antenna itself is developed as a function of time, the problem is identical to that of a static antenna with a phase disturbance along its length.

Establishment of these specifications is not completely straightforward. There are two problem areas. First, the basic criteria from which the specifications are established are essentially arbitrary, and there are several views as to just what phenomena are most important and how they should be defined. Second, the purely mathematical manipulations involved are sufficiently complicated so that the relation between the phase disturbance and the resulting beam distortion can only be exhibited in closed form in a few special cases.

Phase disturbances along a linear antenna will produce two types of beam distortion: (1) degradation of the main lobe, and (2) introduction of side lobes. Degradation of the main lobe is produced by phase disturbances which are relatively slow; that is, by disturbances which do not complete a cycle along the antenna length. Fast disturbances which complete many cycles along the antenna length yield side lobes as their primary product.

In this analysis, assumptions will be made about the nature of the phase disturbance which simplify the mathematical problems as much as possible. The primary such assumption is that the phase disturbance is a Gaussian random process. This assumption is quite reasonable and should not be subject to question or criticism. When the phase disturbance is a random process, the resulting beam pattern will itself be a random process. Actually, the beam pattern perturbations are described by two independent random processes corresponding to real and imaginary components. The properties of these two components could be developed in detail. The approach taken in this analysis is simply to calculate the average value of the perturbed power pattern of the antenna. This approach leads to a relatively straightforward mathematical development which is presented in the Mathematical Appendix to this report.

The resulting average antenna power pattern will possess a loss of main beam gain and an average side lobe level, the magnitudes of which depend upon the properties of the phase disturbance. The approach taken is to require the average power pattern to conform to certain arbitrarily assumed standards.

With respect to the main beam degradation, this approach contains a hidden assumption which should be noted. When the phase disturbance has an average slope across the aperture, the main beam will be deflected. Actual beam broadening and loss of gain is more directly related to an average phase curvature across the aperture. It can be validly argued that random beam deflection, which produces distortion in the final map, should be ignored in determining the main beam gain loss and only the average phase curvature taken into account. This approach was taken in a preliminary study of the problem. In the present analysis, however, random beam deflections are automatically interpreted as a widening of the main beam when the average power pattern is computed. In this sense, the allowable phase disturbance, as it relates to main beam degradation, may be overspecified in this report. The motivation for this approach is that it allows a single and compact mathematical development applicable to both main beam and side lobe aspects of the problem. The specific criterion adopted for allowable main beam degradation is that the average loss in gain at the beam center be less than 3 db. This corresponds to an average beam widening of about 40%, including the effects of random beam deflections, of course.

The side lobe criterion adopted is that the maximum value of the average side lobe level be less than -20db down from the unperturbed main beam. This criterion is essentially arbitrary, adopted on the basis of engineering judgment and experience. An alternative criterion which has a certain amount of merit is to require the integrated side lobe power to be maintained less than a specified value. One problem which arises in specifying side lobe levels is the question of distinguishing between side lobes and the main beam when the wave length of the phase disturbance is about equal to the antenna length. In this case, the vestigual side lobes appear as steps or bumps on the side of the main lobe and the -20 db criterion can be relaxed somewhat. In the Mathematical Appendix, examples of typical average power patterns are illustrated in this critical region.

In order to obtain specific results several additional assumptions have been introduced. One of these relates to the shape of the unperturbed beam pattern. It is assumed to have a Gaussian shape. This, of course, also implies a Gaussian amplitude weighting function. This particular characteristic can often be realized quite closely in a doppler, side-looking system, and its adoption materially simplifies the necessary calculations.

Also, specific forms must be assumed for the spatial spectrum of the phase disturbance. Two types of disturbances will be considered. In the first type, it is assumed that the disturbance is nearly periodic, and the spatial spectrum is a delta-function at the wave number where the phase disturbance power is concentrated. The requirement derived in this case relates to the magnitude of single frequency vibrations which can be allowed. In the second type, it is assumed that the phase disturbance process is a low wave number one with a spatial power spectrum described by a Gaussian function. The necessity of assuming specific forms for the phase power spectrum limits the

applicability of the results to some degree. In particular, the necessity of assuming a finite phase disturbance power could be relaxed. It appears that it is really only necessary to restrict the slope of the phase disturbance to a finite power. In such a case, the phase power spectrum would be indefinitely large at low wave numbers. It is intended to provide this extension of the present results in an addendum to this memorandum.

Cases

Specific stability requirements will be developed for three sets of typical system parameters which essentially represent two distinct cases. Case I employs extreme parameter values representing a future system; case IIa is an intermediate one representing requirements in the immediate future; while case IIb represents requirements of current systems. The parameters for these cases are listed below:

Case I:

V = velocity = Mach 3.0 = 2920 ft/sec
R = range = 40 n.mi. = 2.4×10^5 ft
ℓ = resolution = 6 ft
λ = wave length = 0.1 ft

Case IIa:

V = velocity = Mach 2.0 = 1940 ft/sec
R = range = 20 n.mi. = 1.2×10^5 ft
ℓ = resolution = 12 ft
λ = wave length = 0.1 ft

Case IIb:

V = velocity = Mach 1.0 = 970 ft/sec
R = range = 20 n.mi. = 1.2×10^5 ft
ℓ = resolution = 24 ft
λ = wavelength = 0.1 ft

The general curves in the Mathematical Appendix are expressed in terms of an antenna beamwidth. The doppler filter bandwidth may be taken to represent this beamwidth. A simple and straightforward relation will be supposed between this bandwidth and the other system parameters. A synthetic antenna of length L = VT is supposed where T is the integration time. The azimuth resolution is then simply the beamwidth times the range.

$$\ell = \frac{\lambda R}{2L} = \frac{\lambda R}{2VT} \tag{1}$$

The integration time will thus be

$$T = \frac{\lambda R}{2V\ell} \tag{2}$$

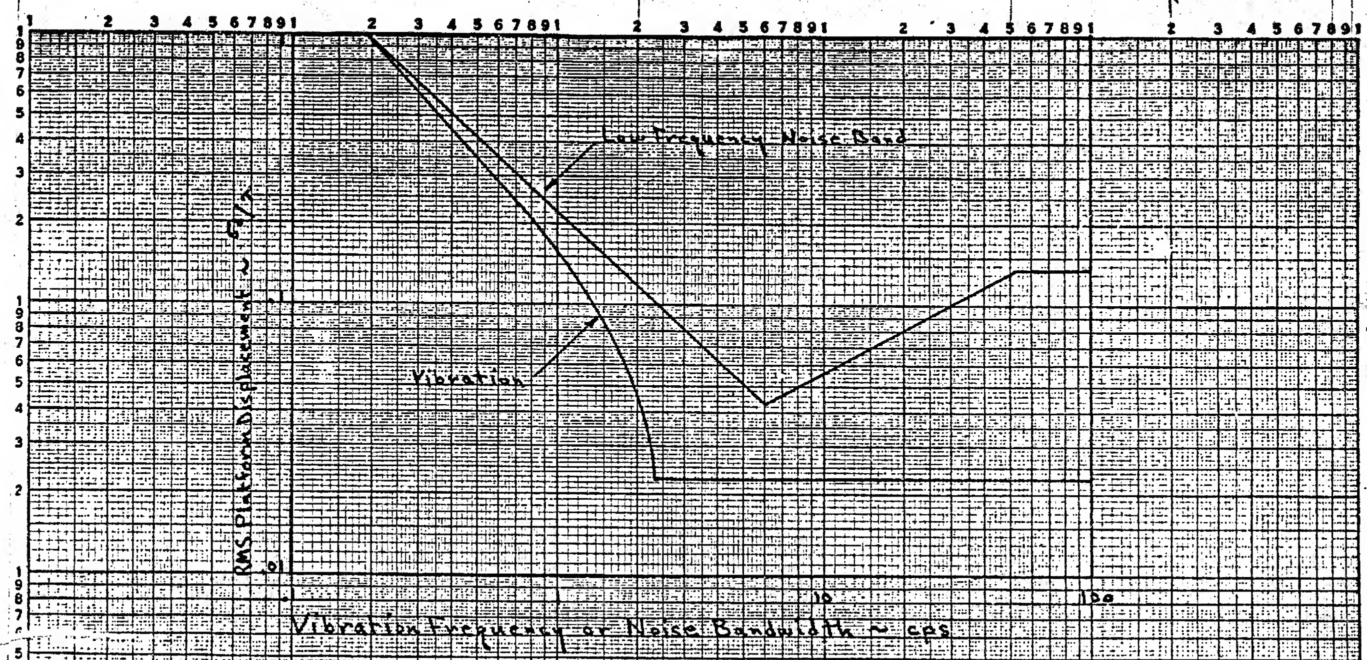

Suggested Platform Stability Requirements for Case I

Figure 1

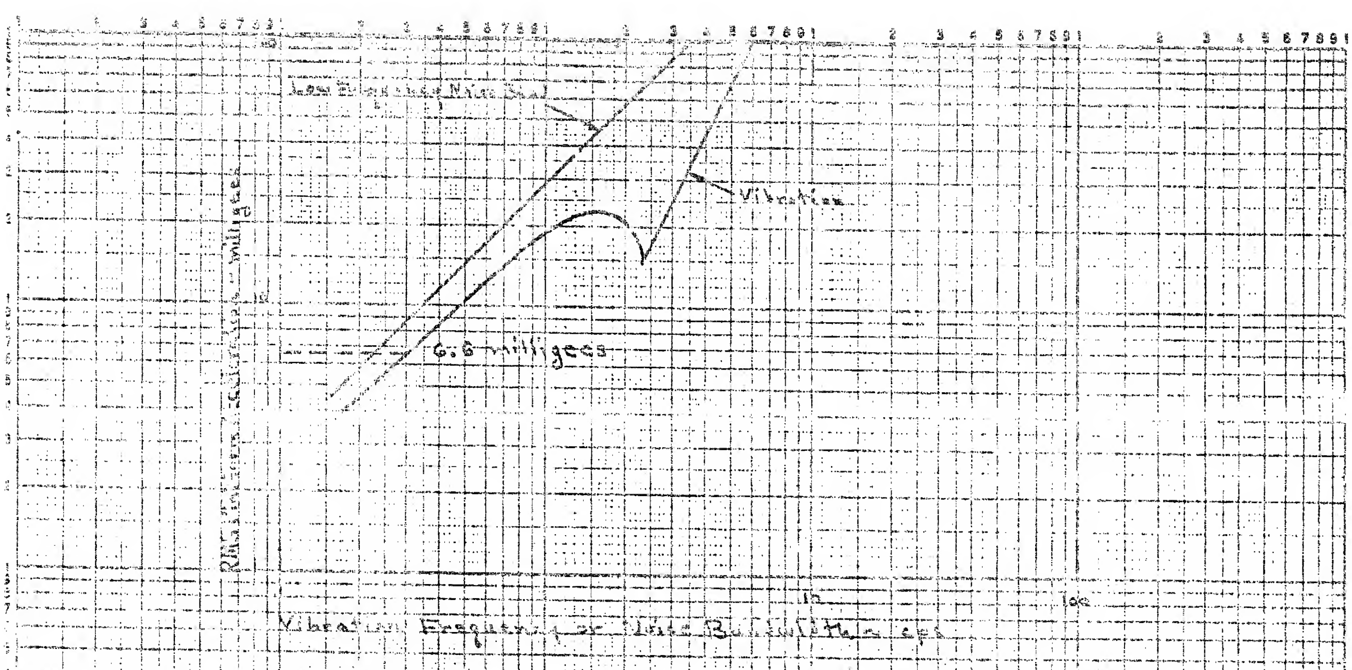

Suggested Platform Stability Requirements for Case I

Figure 2

Sanitized Copy Approved for Release 2010/11/29 : CIA-RDP67B00657R000200180033-1

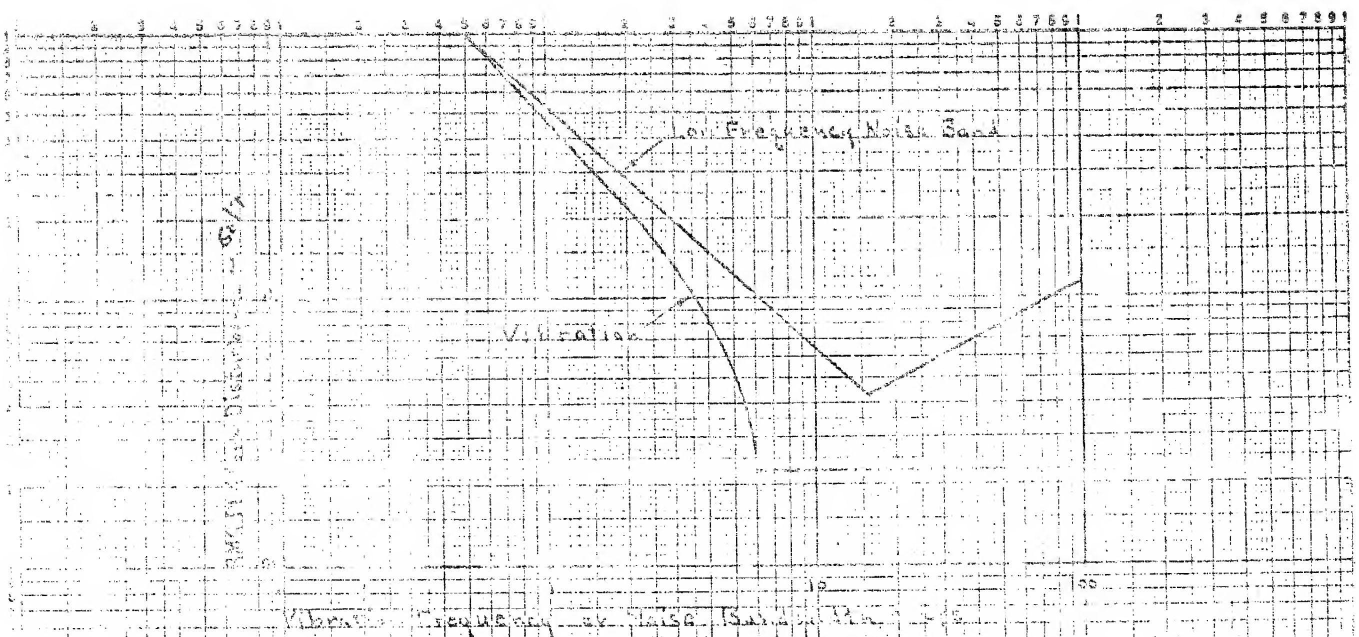

Suggested Platform Stability Requirements for Case II

Figure 3

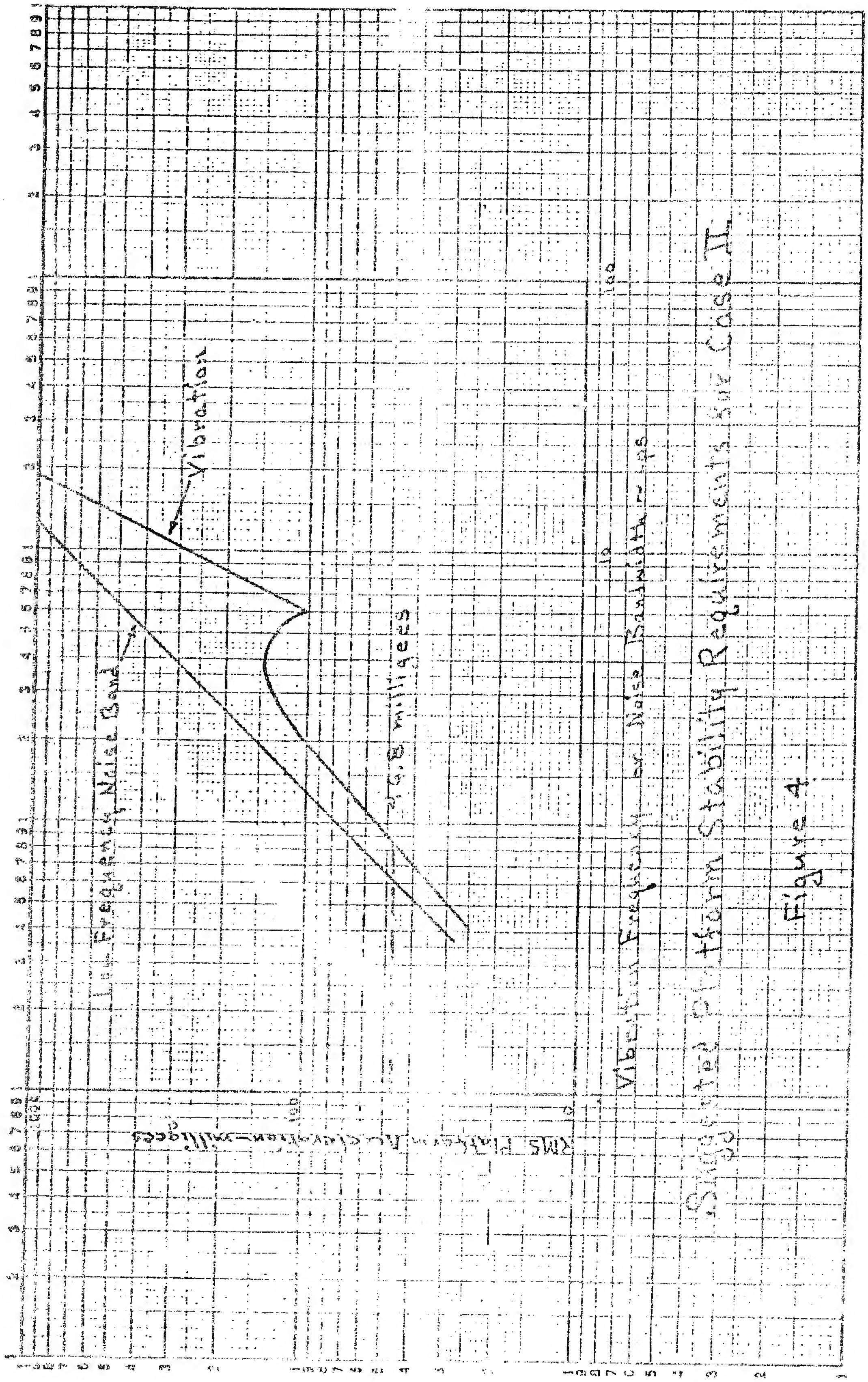

Suggested Platform Stability Requirements for Case II.

Figure 4

For the parameters adopted.

Case I:

$T = .685$ sec

Cases IIa and b:

$T = .258$ sec

The doppler bandwidth (representing the synthetic antenna beamwidth) will be approximately $1/T$ or 1.46 cps and 3.88 cps, respectively, in the two cases.

Platform Stability Requirements

The data in figures 1A and 3A are now easily transformed into specific requirements. Figure 1 shows the allowable rms platform displacement for the two types of disturbances considered in Case I. High frequency periodic disturbances should be maintained less than about 1/50 of a wave length. With the disturbance in a noise band, the rms value should be maintained less than about 1/25 of a wave length in the worst case.

The same data are also plotted in figure 2 where the ordinate is expressed in milligees. In interpreting these latter curves, it must be remembered that it is the displacement spectrum of the noise disturbance which has a Gaussian shape and not the acceleration spectrum. The decrease in allowable acceleration with frequency or noise bandwidth in figure 2 can be attributed to the method of analysis which includes the effect of random wandering of the beam. A previous analysis which only includes the effect of phase curvature on beam broadening arrived at a constant allowable acceleration of 6.6 milligees for a sinusoidal disturbance in the low frequency region in this case. It is suggested that this value be adopted as a lower limit.

Platform stability requirements for Case II are similar. They are shown in figures 3 and 4. As in the first case, a lower limit is suggested in the low frequency region on the basis of studies which considered only the effect of phase curvature. This lower limit is 46.8 milligees.

STALO Stability Requirements

STALO instability manifests itself as a change in wavefront phase during the signal propagation time. The propagation time is

$$\tau = 2R/c \tag{3}$$

The STALO output is represented by

$$\text{STALO output} = \sin\left(2\pi f_c t + \varphi(t)\right) \tag{4}$$

f_c = carrier frequency

$\varphi(t)$ = STALO phase modulation

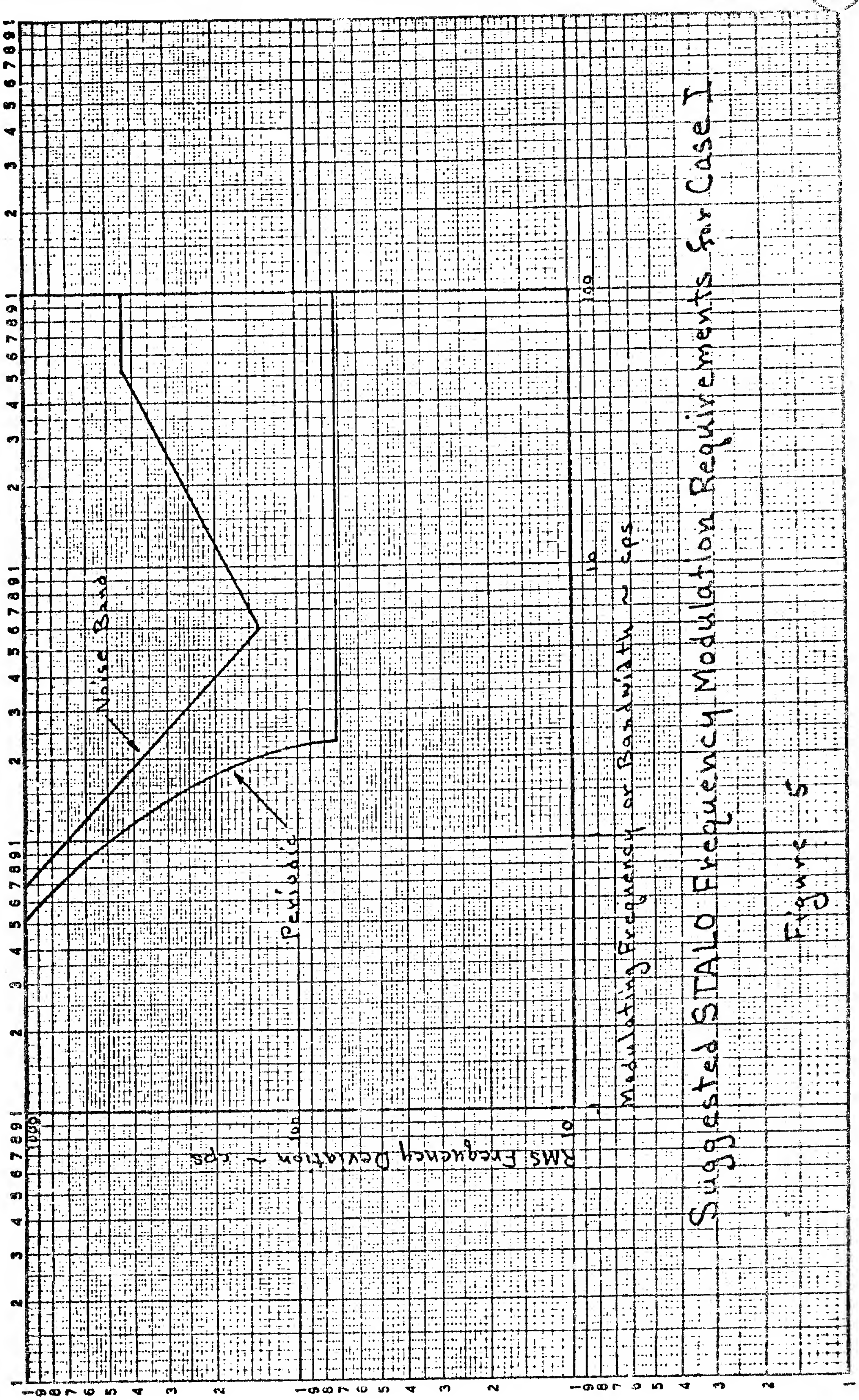

Suggested STALO Frequency Modulation Requirements for Case I

Figure 5

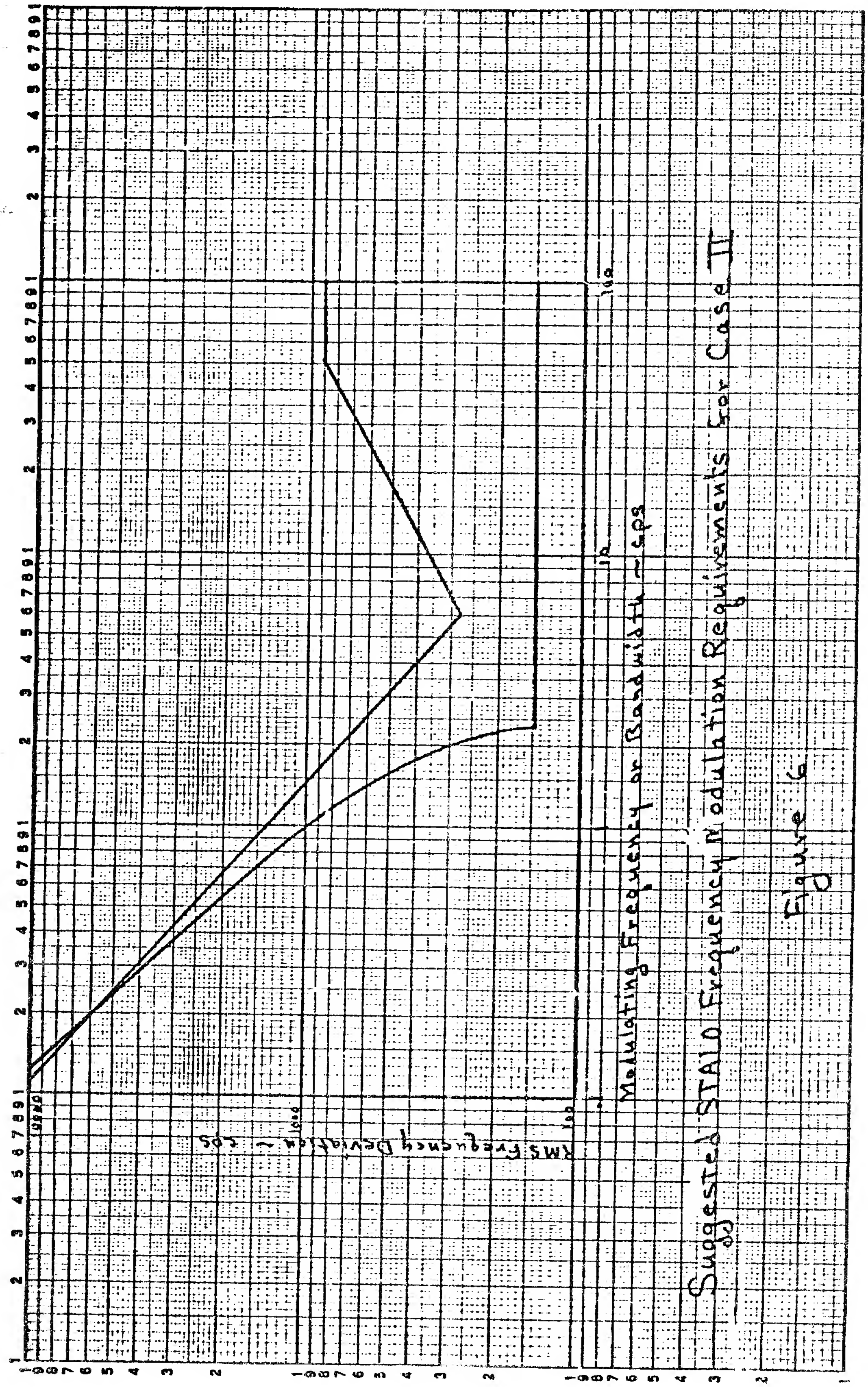

Suggested STALO Frequency Modulation Requirements for Case II

Figure 6

The phase error during the propagation time will be

$$\text{phase error} = \varphi(t) - \varphi(t-\tau) \approx \tau\dot{\varphi}(t) \qquad (5)$$

For R = 40 n.mi., $1/\tau$ = 2KC, and the approximation indicated in equation (5) will be valid out to frequencies on the order of 100 cps.

The quantity $\dot{\varphi}(t)/2\pi$ may be interpreted as a frequency modulation disturbance of the STALO. As before two requirements will be established from the basic results in figures 1A and 3A, one corresponding to a periodic frequency modulation and the other corresponding to a frequency modulation power spectrum of Gaussian form. Figures 5 and 6 show the requirements determined on these bases for the two cases being considered. It should be noted that when the modulating frequency becomes sufficiently large (>1 KC) the approximation in equation (5) is no longer valid, and the allowable frequency deviation increases with the modulating frequency corresponding to a constant deviation ratio.

MATHEMATICAL APPENDIX

Allowable Random Phase Fluctuations Along a Linear Antenna

An antenna pattern is defined in terms of an aperture weighting function.

$$P(\omega) = \int \rho(x)\, e^{i\omega x}\, dx \tag{1A}$$

$$\omega = \frac{4\pi}{\lambda}\theta \tag{2A}$$

$P(\omega)$ = antenna voltage pattern
$\rho(x)$ = antenna weighting function
x = distance along the antenna
θ = look angle
ω = angular wave number
λ = wave length

Since $P(\omega)$ and $\rho(x)$ are Fourier transforms,

$$\rho(x) = \frac{1}{2\pi}\int P(\omega)\, e^{-i\omega x}\, d\omega \tag{3A}$$

Normally, both $\rho(x)$ and $P(\omega)$ will be real and even, and this is supposed the case here.

A phase disburbance along the antenna will be denoted by $\varphi(x)$. This phase disturbance is derived from a displacement disturbance, $d(x)$.

$$\varphi(x) = \frac{4\pi}{\lambda} d(x) \tag{4A}$$

The disturbance $\varphi(x)$ is supposed a stationary Gaussian random process. The autocorrelation and spatial power density spectrum derived from this process are denoted by $\sigma_\varphi^2 \rho(x)$ and $\Phi(\omega)$, respectively.

$$\sigma_\varphi^2 \rho(x_1 - x_2) = \overline{\varphi(x_1)\varphi(x_2)} \tag{5A}$$

$$\Phi(\omega) = \sigma_\varphi^2 \int \rho(x)\, e^{i\omega x}\, dx$$

$$\sigma_\varphi^2 \rho(x) = \frac{1}{2\pi}\int \Phi(\omega)\, e^{-i\omega x}\, d\omega \tag{6A}$$

(7A)

The disturbed voltage pattern is represented by

$$A(\omega) = \int p(x)\, e^{i\omega x + i\varphi(x)}\, dx \tag{8A}$$

$A(\omega)$ is itself a random process. It will be sufficient to consider only the average power pattern.

$$\overline{|A(\omega)|^2} = \iint p(x_1)\, p(x_2)\, \overline{e^{i\varphi(x_1) - i\varphi(x_2)}}\, e^{i\omega(x_1 - x_2)}\, dx_1\, dx_2 \tag{9A}$$

It can be shown that

$$\overline{e^{i\varphi(x_1) - i\varphi(x_2)}} = e^{-\sigma_\varphi^2 (1 - \rho(x_1 - x_2))} \tag{10A}$$

$$\overline{|A(\omega)|^2} = \iint p(x_1)\, p(x_2)\, e^{-\sigma_\varphi^2 (1 - \rho(x_1 - x_2)) + i\omega(x_1 - x_2)}\, dx_1\, dx_2 \tag{11A}$$

This expression will be evaluated for two special cases. In the first, $\varphi(x)$ is supposed very nearly periodic. In the second, $\varphi(x)$ is supposed a low wave number process with a Gaussian spectrum.

When $\varphi(x)$ is nearly periodic or concentrated at the wave number ω_0 ,

$$\rho(x_1 - x_2) = \cos \omega_0 (x_1 - x_2) \tag{12A}$$

$$e^{-\sigma_\varphi^2 \cos \omega_0 (x_1 - x_2)} = \sum_{-\infty}^{\infty} I_K(\sigma_\varphi^2)\, e^{iK\omega_0 (x_1 - x_2)} \tag{13A}$$

$$\overline{|A(\omega)|^2} = \iint P(u)\, P(v)\, du\, dv\, \frac{e^{-\sigma_\varphi^2}}{(2\pi)^2} \sum_{-\infty}^{\infty} \iint I_K(\sigma_\varphi^2)\, e^{iK\omega_0(x_1 - x_2) - iux_1 - ivx_2 + i\omega(x_1 - x_2)}\, dx_1\, dx_2 \tag{14A}$$

$$\overline{|A(\omega)|^2} = e^{-\sigma_\varphi^2} \sum_{-\infty}^{\infty} I_K(\sigma_\varphi^2)\, P^2(\omega + K\omega_0) \tag{15A}$$

A specific form will be assumed for $P(\omega)$. It is supposed that it is Gaussian.

$$P(\omega) = e^{-\frac{\omega^2}{2B^2}} \tag{16A}$$

$$B = .6 \text{ (beamwidth in angular wave numbers)} \tag{17A}$$

For a periodic disturbance, then, the average antenna power pattern will be

$$\overline{|A(\omega)|^2} = e^{-\sigma_\varphi^2} \sum_{-\infty}^{\infty} I_k(\sigma_\varphi^2)\, e^{-\frac{(\omega + k\omega_1)^2}{B^2}} \tag{18A}$$

In the second case, $\Phi(\omega)$ is assumed to have a Gaussian form.

$$\Phi(\omega) = \frac{\sqrt{4\pi}\,\sigma_\varphi^2}{\beta} e^{-\frac{\omega^2}{\beta^2}} \tag{19A}$$

$$\sigma_\varphi^2 \rho(x) = \sigma_\varphi^2 e^{-\frac{\beta^2 x^2}{4}} \tag{20A}$$

$$\beta = 1.2 \text{ (disturbance bandwidth in angular wave numbers)} \tag{21A}$$

The integrand in equation (11A) will now include the following factor

$$e^{-\sigma_\varphi^2(1-\rho(x_1-x_2))} = e^{-\sigma_\varphi^2\left(1 - e^{-\frac{\beta^2(x_1-x_2)^2}{4}}\right)} \tag{22A}$$

This rather awkward function can be expanded in a number of ways. The following approximation is convenient and useful.

$$e^{-\sigma_\varphi^2\left(1 - e^{-\frac{\beta^2(x_1-x_2)^2}{4}}\right)} \approx e^{-\sigma_\varphi^2} + (1-e^{-\sigma_\varphi^2})\, e^{-\frac{\sigma_\varphi^2 \beta^2 (x_1-x_2)^2}{4(1-e^{-\sigma_\varphi^2})}} \tag{23A}$$

This approximation is accurate to a few percent for extreme ranges of all the parameters involved. Moreover, when substituted into equation (11A), this expression is readily evaluated. The result of this calculation is

$$\overline{|A(\omega)|^2} \approx e^{-\sigma_\varphi^2} P^2(\omega) + \frac{(1-e^{-\sigma_\varphi^2})^{3/2}}{\sqrt{\pi}\,\sigma_\varphi \beta} \int P^2(u)\, e^{-\frac{(1-e^{-\sigma_\varphi^2})(\omega-u)^2}{\sigma_\varphi^2 \beta^2}}\, du \tag{24A}$$

With the Gaussian form assumed for $P(\omega)$ in equation (16A), this becomes

$$\overline{|A(\omega)|^2} \approx e^{-\sigma_\varphi^2 - \frac{\omega^2}{B^2}} + \frac{(1-e^{-\sigma_\varphi^2})}{\sqrt{1+\frac{\beta^2\sigma_\varphi^2}{B^2(1-e^{-\sigma_\varphi^2})}}} e^{-\frac{\omega^2}{B^2\left(1+\frac{\beta^2\sigma_\varphi^2}{B^2(1-e^{-\sigma_\varphi^2})}\right)}} \qquad (25A)$$

Equations (18A) and (25A) will now be employed to determine specifications for allowable phase deviations. In specifying allowable phase disturbances, two phenomena must be taken into account; (a) deterioration of the main beam, and (b) the magnitudes of random side lobes. Deterioration of the main beam will be specified in terms of an average loss in gain at the beam center. The criterion adopted is that an average loss of 3db can be allowed. This corresponds approximately to a 40% widening of the beam. The criterion adopted for random side lobes is that their average level be less than -20 db below the undistorted main beam. These two criteria will lead to two independent specifications. In general, main beam considerations are determining when the major portion of the phase disturbance have spatial frequencies within the spatial antenna beamwidth, and side lobe considerations are determining when the major portion of the phase disburbance have spatial frequencies greater than the spatial antenna beamwidth.

The case of a periodic phase disturbance is considered first. If σ_φ^2 is supposed small, equation (18A) can be expanded to yield

$$\overline{|A(\omega)|^2} \approx e^{-\frac{\omega^2}{B^2}} + \frac{\sigma_\varphi^2}{2} e^{-\frac{(\omega+\omega_0)^2}{B^2}} + \frac{\sigma_\varphi^2}{2} e^{-\frac{(\omega-\omega_0)^2}{B^2}}, \quad \sigma_\varphi^2 \ll 1 \qquad (26A)$$

With $\omega_0 \gg B$, it is obvious that $\sigma_\varphi^2 < .02$ (radians)^2 to provide side lobes of less than -20 db. This specification is plotted in figure 1A. The abscissa in this curve is the ratio of the spatial frequency of the disturbance, ω_0, to half the spatial antenna beamwidth, $B/1.2$, which is denoted by ν.

$$\nu = \frac{1.2\,\omega_0}{B} \qquad (27A)$$

The magnitude of the main beam center will be

$$\overline{|A(0)|^2} = e^{-\sigma_\varphi^2} I_0(\sigma_\varphi^2) + 2e^{-\sigma_\varphi^2} I_1(\sigma_\varphi^2)\, e^{-\frac{\omega_0^2}{B^2}} + \cdots \qquad (28A)$$

This has been set equal to .5 and the resulting relation between σ_φ^2 and ν calculated. This relation is also plotted in figure 1A. The two specifications have been arbitrarily connected together by a dashed line to provide a complete specification as a function of ν. Points on this connecting line will have side lobes which are somewhat larger than -20 db, but they will be so rudimentary that they appear to be more a part of the main beam than side lobes. A feeling for the shape of typical power patterns can be obtained

from figure 2A where three representative patterns corresponding to points on the connecting specification are plotted.

A similar specification will be derived for the case of a low frequency band of noise as the disturbance. The main beam specification is determined by setting equation (25A) equal to .5 with $\omega = 0$. The specification derived in this manner has been plotted in figure 3A. In this figure the abscissa is taken to be β/B which is the ratio of the noise bandwidth in wave numbers to half the beamwidth in wave numbers. As in the previous case, the abscissa is denoted by ν.

The sidelobe specification is obtained by approximating equation (25A) for small σ_φ^2. If, in addition, $\beta \gg B$, the sidelobe specification is given by

$$\frac{\sigma_\varphi^2}{\sqrt{1+\beta^2/B^2}} = \frac{1}{100} \qquad (29A)$$

This relation is also plotted in figure 3A. The two specifications are arbitrarily connected together as indicated by the dashed line.

In order to give a feeling for the shape of average power patterns, particularly on the connecting specification, patterns for three representative cases are shown in figure 4A.